

# Improved regional algorithm to retrieve total suspended particulate matter using IRS-P4 ocean colour monitor data

Yaswant Pradhan<sup>1</sup>, A V Thomaskutty<sup>2</sup>, A S Rajawat<sup>2</sup> and Shailesh Nayak<sup>2</sup>

<sup>1</sup> School of Earth, Ocean and Environmental Sciences, University of Plymouth, Plymouth PL4 8AA, UK

<sup>2</sup> Marine and Water Resources Group, ISRO-Space Applications Centre, Ahmedabad 380 015, India

E-mail: [yaswant.pradhan@plymouth.ac.uk](mailto:yaswant.pradhan@plymouth.ac.uk)

Received 27 February 2005, accepted for publication 4 April 2005

Published 21 June 2005

Online at [stacks.iop.org/JOptA/7/343](http://stacks.iop.org/JOptA/7/343)

## Abstract

Data from seven validation campaigns in the coastal waters of the Bay of Bengal (BOB) were used to develop a regional SPM (suspended particulate matter) algorithm. The *in situ* data sets for this algorithm are obtained from 86 stations with optical and 68 stations with total SPM measurements encompassing SPM concentrations between 10 and 189 mg l<sup>-1</sup>, where most of the observations are in shallow (case 2, average depth ~45 m) waters and a limited number of samples in open case 1 waters. From simple statistical analyses we found a close relationship between SPM concentration and diffuse attenuation coefficient at 555 nm ( $K_{555}$ ) in the BOB coastal waters. The linear regression to the fit has a coefficient of determination ( $r^2$ ) 0.96 with a standard error of estimates ( $\sigma$ ) 12.5 mg l<sup>-1</sup> for the above SPM range. The algorithm relating  $K_{555}$  to  $[L_{wn443}/L_{wn670}]$  has been evaluated through a regression analysis of radiometric profiles in the BOB. However, the new SPM algorithm overestimates in case 1 waters (SPM range 0.05–25.0 mg l<sup>-1</sup>), where a spectral reflectance ratio algorithm (Tassan 1994 *Appl. Opt.* **33** 2369–78) appears to produce better results. An integration of both the approaches performs better in generating the routine IRS-P4 OCM (ocean colour monitor) SPM mapped product.

**Keywords:** Bay of Bengal, SPM, diffuse attenuation coefficient, ocean colour, case 2 water

(Some figures in this article are in colour only in the electronic version)

## 1. Introduction

Accurate physical, biological and chemical measurements of the upper-ocean are essential for understanding the structures and processes that affect the climate and environment. Ocean colour observation with remote sensors from air and space platforms has become popular over the last few decades because of its continuous coverage of the earth surface, which allows for the identification of zones characterized by physical and biological processes occurring at the sea surface. Ever since the launching of the CZCS (coastal zone color

scanner), mapping and quantitative estimation of the surface bio-geophysical constituents such as chlorophyll-a, suspended particulate material (SPM), and gelbstoff (coloured dissolved organic matter or CDOM), through the remote sensing of ocean colour has gone through a quiet revolution. Extensive studies have been carried out to relate explicitly radiance/reflectance with in-water constituents over the past three decades (Morel and Prieur 1977, Gordon *et al* 1988, Sathyendranath *et al* 1994, Lee *et al* 1998). Previous studies confirm that for case 1 waters (devoid of direct influence of land runoff and littoral drift), most of the observed variations in the colour and transparency can

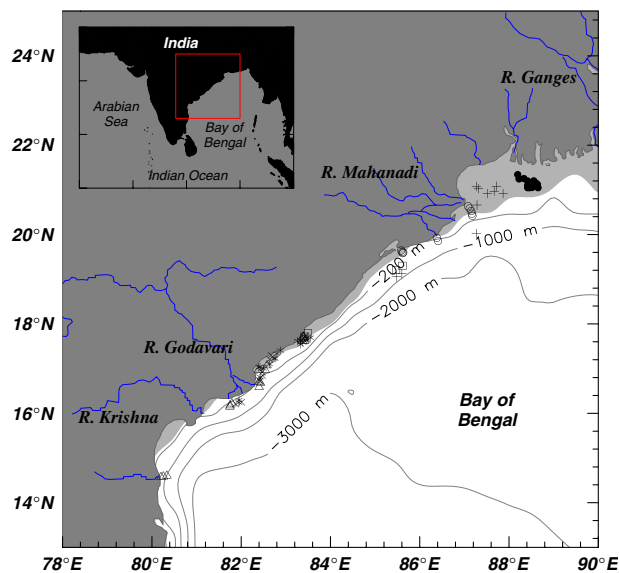


**Figure 1.** Study area—the Bay of Bengal coastal waters. Major river systems and bathymetry contours for 200 m, 1, 2 and 3 km (<50 m depth is shaded) are overlaid. CCDB data points used for this study are shown as different symbols for different cruises (see table 1).

be related to varying concentration of marine phytoplankton and their decay products (CDOM). But the presence of highly variable contributions of suspended sediment and minerals by river discharge and the presence of exceptionally higher pigment and CDOM concentration makes the coastal (case 2) waters more optically complex. In addition the global colour ratio algorithms break down in the case 2 regime because of the presence of multiple substances, which do not co-vary with chlorophyll concentration.

The Bay of Bengal is a region of large freshwater and sediment input (Emmel and Curray 1984), high sea-surface temperature and variable monsoonal forcing. The annual fresh water discharge into the Bay exceeds  $1.5 \times 10^{12} \text{ m}^3$ , which reduces the mean salinity by about 7‰ in the northernmost bay (Laviolette 1967). The bay receives about  $2 \times 10^9$  ton of sediments annually, mostly contributed through the Himalayan Rivers—the *Ganges* and the *Brahmaputra* (G–B) from the north (figure 1); the Indian Peninsular Rivers—the *Mahanadi*, the *Godavari*, the *Krishna*, etc from the west; and the *Irrawady* and the *Salween* from the east. It is therefore worth investigating the state of the distribution of surface particulate matters and their consequences over the bay. In the present context, we derive a new method to estimate SPM concentration from remotely sensed optical signals.

The ocean colour monitor (OCM) onboard IRS-P4 (Oceansat-1) is designed to record the reflected radiance from the earth which in turn can be used to estimate the concentrations of chlorophyll-a, SPM and gelbstoff at the sea surface and atmospheric aerosol in the marine environment (see Anonymous 2003 for technical specifications). Originally, the SPM retrieval algorithm using OCM data followed a similar approach outlined by Tassan (1994), tuned for Indian waters, which is valid for lower SPM concentrations within 30% (Anonymous 2003). To validate/modify this approach in coastal (case 2) waters, the

SAC (Space Applications Centre) and GSI (Geological Survey of India) conducted six campaigns in the coastal waters of the Bay of Bengal during 2000–2002. From these observations we found that it makes sense to calibrate the ocean colour algorithms in terms of the diffuse attenuation coefficient,  $K$ , in the Bay of Bengal coastal waters. Based on the *in situ* measurements, we observed that SPM concentrations in the coastal BOB are highly correlated with  $K_{555}$ , and propose a site-specific SPM algorithm with a standard error of estimates  $15 \text{ mg l}^{-1}$ . Since most of the *in situ* samples were obtained within the continental margin (average depth of  $\sim 45 \text{ m}$ ), we retain the old (Tassan 1994) approach which is valid for deeper waters ( $>50 \text{ m}$  depth) where we have very sparse measurements during these campaigns.

## 2. Measurements and model description

The coastal cruise database (CCDB) is composed of seven OCM validation campaigns (joint ISRO–GSI and NRSA–ILS) in the Bay of Bengal during 2000–2002, onboard R V *Samudra Kaustubh*. All of the cruises were carried out between December and April to accumulate a total number of 86 optics stations out of which SPM sampling were taken for 68 stations; a brief summary of campaign periods and measurements relevant to this paper are shown in table 1. Data for total SPM, chlorophyll-a and optical parameters from over the continental margin (8.8–775 m with an average depth of  $\sim 45 \text{ m}$ ), off the east coast of India (between  $80.20^\circ\text{E}$ ,  $14.6^\circ\text{N}$  and  $88.65^\circ\text{E}$ ,  $21.34^\circ\text{N}$ ) were used to examine the variation in optical properties with varying SPM and chlorophyll concentrations. Over this region the sediment loads are very high (between 13 and  $189 \text{ mg l}^{-1}$ ), particularly at the head of the bay and at the river mouths, and phytoplankton pigment concentrations are moderately low ( $0.01$ – $1.84 \mu\text{g l}^{-1}$ , from CCDB). Hence the changes in optical quantities are basically dominated by inorganic sediments carried by major river systems in this region (figure 1).

### 2.1. Suspended particulate matter

Water samples were collected at multiple depths (0–0.5, 5, 10 and 15 m) during all cruises, except ST-140 collected only at 0–0.5 m depth since the water column was well-mixed, using winch operated Niskin bottles. The vertical distributions of the sediments within the shallow well mixed coastal waters are relatively uniform over the top few metres, especially near the mouth of the *Ganges* where the sediment load is maximum, accompanied by a good mixing of the water column by strong semi-diurnal tidal currents. Suspended particulate materials (dry weight in  $\text{mg l}^{-1}$ ) were determined gravimetrically as outlined in Strickland and Parsons (1972) and as specified in JGOFS protocols (UNESCO 1994). Samples were filtered through  $0.4 \mu\text{m}$  pre-weighted polycarbonate filters. The filters were washed with three 2.5–5 ml aliquots of distilled water and immediately dried in an oven at  $75^\circ\text{C}$ . The filters were then reweighed in the laboratory using an electro-balance.

### 2.2. Optical measurements

Measurements of the underwater light field were performed with (i) a LI-COR portable underwater spectro-radiometer,

**Table 1.** Coastal cruise database summary showing only the periods, extents and numbers of optics and SPM stations.

Cruise	Duration	Optics (no. of observations)	SPM (no. of observations)	Geographical extent
ST-133 (+)	13 Jan 2000	LI-COR	Multi-depth	85.60°–87.86°E
	22 Jan 2000	(09)	(09)	19.13°–21.08°N
ST-136 (*)	29 Mar 2000	LI-COR	Multi-depth	81.95°–83.55°E
	6 Apr 2000	(18)	(17)	16.24°–17.71°N
ST-140 (●)	20 Dec 2000	SPMR/SMSR	Sub-surface	88.19°–88.65°E
	24 Dec 2000	(15)	(15)	21.04°–21.34°N
ILS-03 (○)	4 Mar 2001	SPMR/SMSR	Nil	85.58°–87.18°E
	6 Mar 2001	(12)		19.58°–20.63°N
ST-142 (△)	19 Mar 2001	SPMR/SMSR	Multi-depth	80.20°–83.42°E
	24 Mar 2001	(17)	(16)	14.59°–17.74°N
ST-149 (□)	31 Jan 2002	SPMR/SMSR	Nil	83.41°–85.61°E
	1 Feb 2002	(04)		17.71°–19.30°N
ST-151 (×)	3 Mar 2003	SPMR/SMSR	Multi-depth	81.87°–83.47°E
	8 Mar 2003	(11)	(11)	16.21°–17.74°N
Total observations		86	68	

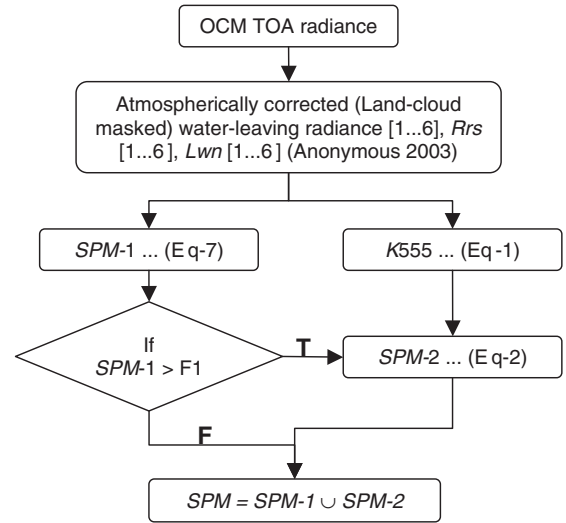
Sub-surface = 0–0.5 m depth; for SPMR/SMSR and multi-depth see text sections 2.1 and 2.2

(ii) a SeaWiFS profiler multi-channel radiometer (SPMR), and (iii) a SeaWiFS multi-channel surface reference (SMSR). These instruments are basically designed to collect photons travelling in specific directions (upward/downward), which can be converted into physical values (namely spectral irradiance, radiance). LI-COR measures the upwelling irradiance ( $E_u(z, \lambda)$ ) and downwelling irradiance ( $E_d(z, \lambda)$ ) within the wavelength domain 350–900 nm (continuous 1 nm interval). SPMR profiles both upwelling radiance ( $L_u(z, \lambda)$ ) and downwelling irradiance ( $E_d(z, \lambda)$ ), and SMSR measures the above surface incoming solar irradiance ( $E_s(O^+, \lambda)$ ) using DSP techniques and 24 bit A/D converters in seven spectral channels (central wavelength [bandwidth] in nm: 412 [10], 443 [10], 490 [10], 510 [10], 555 [10], 670 [20], 780 [20]) (Satlantic User's Manual 2000). The optical sensor characteristics of the Satlantic radiometer are akin to the OCM (Anonymous 2000). The apparent optical properties like spectral water-leaving radiance ( $L_w(\lambda)$ ), remote sensing reflectance ( $R_{rs}(\lambda)$ ), normalized water-leaving radiance ( $L_{wn}(\lambda)$ ) and diffuse attenuation coefficient ( $K(\lambda)$ ) were computed (see appendix) following the theory (Mobley 1994) and standard protocols (Mueller 2000).

Light radiance and irradiance fields decrease exponentially with depth under typical conditions for which incident lighting is provided by the sun and the sky. This effect is expressed as another apparent optical property called the spectral diffuse attenuation coefficient (expressed as  $K(\lambda)$ ). The method described in Mueller and Austin (1995) is a general practice of estimating the  $K$  profiles (see appendix, equation (A.1)). Alternatively they can also be related to upwelling radiance ratios (Austin and Petzold 1981). The diffuse attenuation coefficient  $K$  555 can be related to the ratio of normalized water-leaving radiance [ $L_{wn}443/L_{wn}670$ ] as

$$\ln[K 555 - 0.07] = \ln(A) + B \ln \left[ \frac{L_{wn}443}{L_{wn}670} \right] \quad (1)$$

where  $A$  and  $B$  are the regression coefficients, and the attenuation coefficient for pure water,  $K_w555 = 0.07 \text{ m}^{-1}$ , is the minimum possible value for  $K$  555 (Jerlov 1976).

**Figure 2.** Schematic of the integrated model flow.

The calibrated single component algorithm for SPM in terms of diffuse attenuation coefficient  $K$  555 in turbid coastal waters may be expressed as

$$\text{SPM2} = mK(555) + n \quad (2)$$

where  $m$  and  $n$  are the slope and intercept of the linear regression, respectively.

The final product (SPM) in the current discussion is the integration of values below and above a case 1 flag ( $F1 = 25.5$ ) from SPM1 (Tassan 1994) and SPM2 respectively. In the new model this option is user specific and can be adjusted for different regions. We have opted for this value for the Bay of Bengal because of two basic reasons:

- (i) the existing Tassan algorithm was reportedly working well in relatively less turbid waters (Chauhan 2002), as we shall see in the results and discussions section, and
- (ii) the statistics of *in situ* SPM data show that this is a typical value where bathymetry is shallower than 50 m.

A schematic of the flow is given in figure 2.

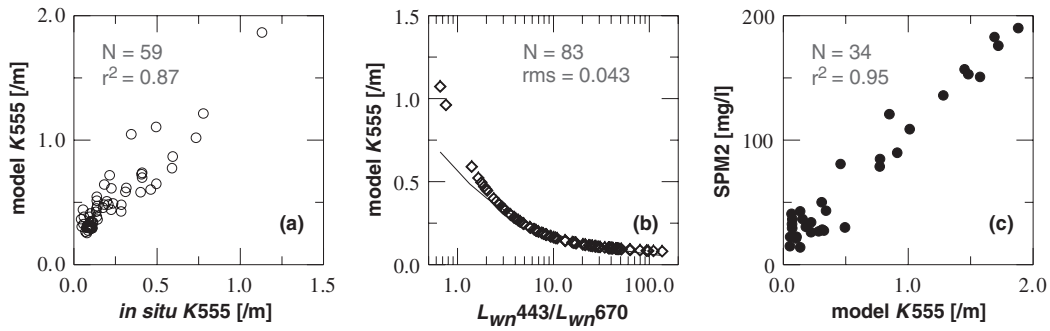


**Figure 3.** Scattergrams of (a) *in situ*  $K555$  and model  $\hat{K}555$ ; data from ST-133 and ST-136 are excluded in the graph, (b) logarithmic scaling *in situ* water-leaving radiance ratio  $[L_{wn443}/L_{wn670}]$ , and model  $\hat{K}555$  (linear) (c) model  $\hat{K}555$  versus SPM2; one half of the data is extracted from a normally distributed sample.

### 3. Results and discussions

In water diffuse attenuation coefficients can be calculated from *in situ* profiles of spectral irradiance and radiance field (equation (A.1)). However, this is not possible from satellite measurements as it provides information at a single layer. Therefore, we propose an indirect method (similar to Austin and Petzold 1981) to estimate the in-water diffuse attenuation coefficients by establishing an empirical relationship with ratios of normalized water-leaving radiances, based on direct comparison with *in situ* radiometric profiles. Data from CDDB were combined to bring together a regression sample of size  $N = 59$  (only SPMR stations). We have excluded ST-131 and ST-136 data from the initial calibration of  $K$  and  $L_{wn}$  ratio. By doing so, we avoid the possible discrepancies due to the differences in measurement methods (single depth LICOR and continuous profiling SPMR), in configuring the basic relationship. Unfortunately, there is no collocated LICOR-SPMR measurement available to examine the difference; nevertheless, the calibrated spectral shapes do not depart drastically from each other in laboratory environments. The linear least-squares fit to this data is

$$\ln[K555 - 0.07] = -0.356251 - 0.871654 \ln\left[\frac{L_{wn443}}{L_{wn670}}\right] \quad (3)$$

with coefficient of determination  $r^2 = 0.87$ , and a residual standard deviation of 0.226 (in log space).  $K555$  in equation (3) was estimated from the irradiance profiles as explained in (A.1). The linear relationship between *in situ* and model  $\hat{K}555$  is shown in figure 3(a).

In the next step, most of the data (83 out of 86) were included to evaluate the new relationship. All LI-COR spectra were split and integrated (convoluted) to match the SPMSR/SMSR bandwidths before the calculation of higher-level parameters. The new formulation following equation (3) can be transformed as

$$\hat{K}555 = 0.07 + 0.7003 \left[\frac{L_{wn443}}{L_{wn670}}\right]^{-0.87} \quad (4)$$

with a standard error of estimate  $\sigma = 0.043 \text{ m}^{-1}$  ( $N = 83$ ;  $r^2 = 0.95$ ), which is calculated as

$$\sigma = \sqrt{\frac{\sum_{n=1}^N [\hat{K}555 - K555]^2}{N - 2}} \quad (5)$$

where  $K555$  is the diffuse attenuation coefficients calculated from *in situ* irradiance profiles and  $\hat{K}555$  is the model estimation from normalized water-leaving radiance (using equation (4)). Figure 3(b) illustrates the regression fit of the modelled  $\hat{K}555$  and  $[L_{wn443}/L_{wn670}]$ .

About half of the samples from a normal distribution (slightly biased toward higher SPM concentrations) were taken to establish the empirical relationship between model  $\hat{K}555$  and measured *in situ* SPM is formulated, using equation (2), as:

$$\text{SPM2} = (93.2 \times \hat{K}555) + 13.24 \quad (6)$$

with a standard error of estimates  $15 \text{ mg l}^{-1}$ , for  $25 < \text{SPM2} < 200 \text{ mg l}^{-1}$  ( $N = 34$ ). Scatter at different levels of SPM are shown in figure 3(c), where large discrepancies are observed at lower SPM concentrations. The physical limitations of lone use of this approach, however, are twofold:

- (i) this model consistently overestimates SPM concentrations in open ocean waters, the lowest possible SPM that can be retrieved using this model is  $\sim 25 \text{ mg l}^{-1}$ , and
- (ii) application of this approach to OCM restricts an accurate estimate of SPM values greater than  $216.517 \text{ mg l}^{-1}$  since the  $[\frac{L_{wn443}}{L_{wn670}}]$  saturates at  $\sim 0.2813$ .

Therefore, a combination of the existing case 1 SPM model to this new method is believed to produce better results. The case 1 SPM algorithm (SPM1) for OCM is a fine-tuning of Tassan's approach in Indian waters (Anonymous 2003):

$$\text{SPM1} = 25 \exp\left(a_0 + a_1 \left[ (Rrs(555) - Rrs(670)) \times \left(\frac{Rrs(555)}{Rrs(490)}\right) \right]\right) \quad (7)$$

where  $0 < \text{SPM1} < 25 \text{ mg l}^{-1}$ ;  $a_0 = 2.166$ ;  $a_1 = 0.991$ .

Figure 4 illustrates the scatter of *in situ* and model SPM concentrations for all test data sets from CCDB (sample size  $N = 68$ ). SPM1 explains 74% of the total variance (figure 4(a)); the RMS error is very high ( $57.17 \text{ mg l}^{-1}$ ). While SPM1 fails to estimate the higher concentrations, SPM2 performs relatively better ( $r^2 = 0.93$ , RMS = 15.5) but overestimates all values lower than  $\sim 25 \text{ mg l}^{-1}$  (figure 4(b)). An initial guess of 25.5 threshold value between SPM1 and SPM2 improves the overall result of SPM explaining 97% of the variance with an RMS = 12.51 (figure 4(c)). The maximum

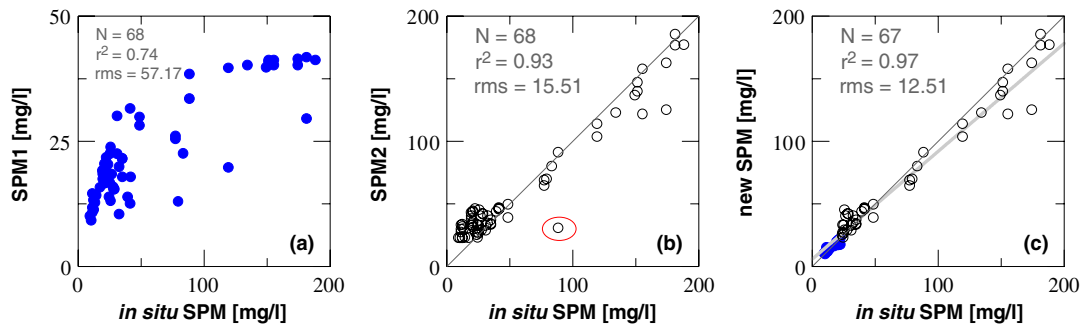


**Figure 4.** Comparison of *in situ* SPM with model derived SPM: (a) *in situ* versus SPM1, (b) *in situ* versus SPM2 (one outlier detected within the ellipse) and (c) *in situ* versus integrated SPM (one outlier has been removed). Note that SPM1 strongly undermines the higher concentrations, whereas SPM2 overestimated the lower values. For the test data-sets, the integrated approach performs better than any stand-alone model. The thick grey line in (c) is a linear fit to the data showing small bias at higher concentrations.

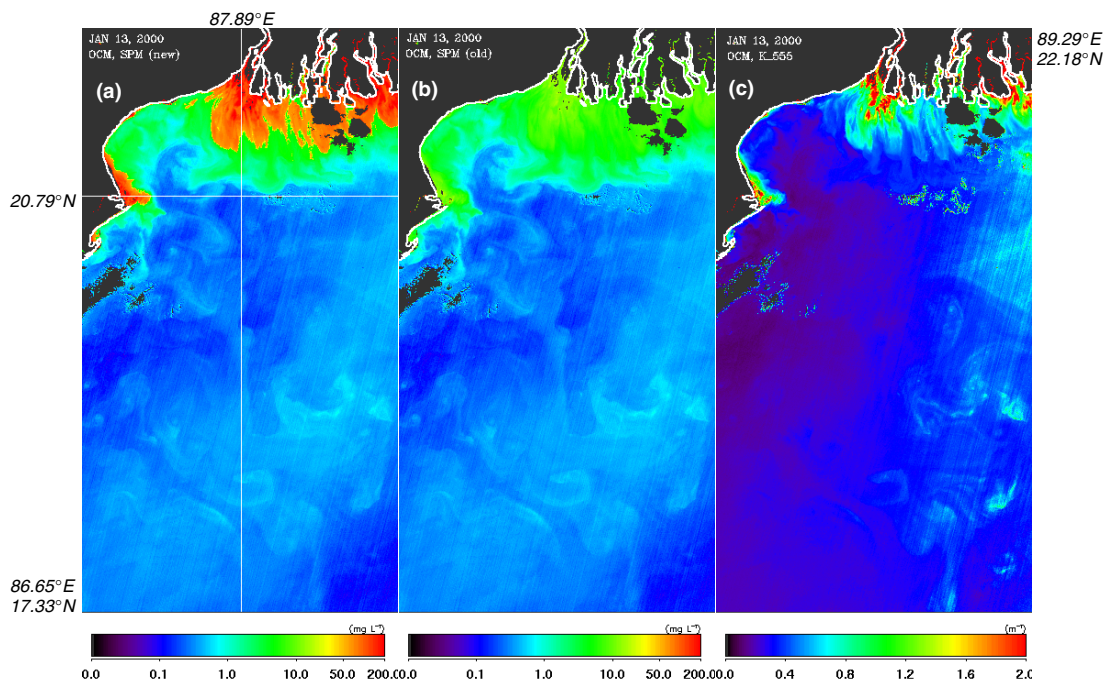


**Figure 5.** Model output using 13 January 2000 IRS-P4 OCM data (17.33°–22.18°N to 86.65°–89.29°E): (a) SPM with the new integrated approach, (b) SPM using the old algorithm and (c)  $\hat{K}555$  with the new approach (as in equation (4)).

deviations from the regression fit occur at the border of the threshold value apart from a few outliers. When applied to OCM the difference between the old algorithm and the new approach was quite apparent off river mouths, especially off the *Ganges–Brahmaputra* deltaic regions (figures 5(a) and (b)). SPM distribution in this region is highly dynamic and the cross-shelf excursion of turbid waters is often synchronized with the tide cycle. Therefore, the next objective to implement the current approach would be to monitor the influence of tidal cycle on the optical properties and the evaluation of the performance of all possible approaches. Nevertheless, the  $\hat{K}555$  thus derived from OCM depicts not only the spatial patterns but also the extent and changing directions of the shallow water shoals (figure 5(c)) which would be quite vital for both environmental and commercial (e.g. qualitative ship routing) applications.

### 3.1. Validation match-ups

CCDB data from ST-151 and a few points from the ST-131 cruise, which were not included in the initial calibration procedure, are being used to evaluate the performance of the new approach. Comparisons between OCM derived and *in situ* SPM are shown in table 2. Most of the match-up points fall within the SPM1 domain except for 15 December 2000; therefore, most of the match-up points mimic the SPM1 results. Although the numbers of co-located points are not sufficient (because the OCM repeats the area every two days and sometimes the *in situ* locations are cloudy for overpass timing) to claim the complete validity of the model on OCM data, this is one step forward towards establishing a regional model for ocean colour parameters.

**Table 2.** Comparison of *in situ* SPM with OCM derived SPM using different methods.

Date ddmmyy	<i>In situ</i> SPM (mg l <sup>-1</sup> ) TO [hh:mm]	OCM <sup>a</sup> SPM1 (mg l <sup>-1</sup> )	OCM SPM2 (mg l <sup>-1</sup> )	New OCM SPM (mg l <sup>-1</sup> )	Remarks
13012000	27 [14:00]	05.789	22.7	05.789	Water depth 775 m
15012000	20.2 [12:30]	10.291	27.391	27.391	Water depth 22.89 m
03032002	14 [11:30]	12.572	22.482	12.572	Clear sky
03032002	15 [13:30]	13.973	29.134	13.973	Clear sky
04032002	12 [12:00]	10.579	28.984	10.579	OCM pass March 3
04032002	12 [14:20]	11.594	22.071	11.594	OCM pass March 3
05032002	13 [11:45]	18.153	30.926	18.153	Cloudy
05032002	11 [14:35]	09.012	21.998	09.012	Partly cloudy
07032002	12 [11:40]	16.344	26.609	16.344	Cloudy
07032002	10 [13:43]	15.853	22.100	15.853	Partly cloudy

<sup>a</sup> OCM overpass for all dates—12:00 noon local standard time. TO—time of observation.

#### 4. Outlook

The main objective of this experiment was to evaluate a regional model to predict the SPM concentration in the highly turbid zones in the Bay of Bengal. The initial outcomes are encouraging, however, we need more *in situ* observations in both coastal and oceanic waters to evaluate the presumption in case 1 waters. Because the sky remains highly obscured by the monsoon clouds and the sea conditions are unfavourable, the number of ocean colour validation campaigns during the summer monsoon period (June–September) is almost zero. The present strategy leaves more than a 50% gap in observations along the time domain and our understanding about the complete range of the annual cycle (from ocean colour observation) of the sediment loads in the Bay. In this paper we have assumed that the changes in optical properties are largely dominated by inorganic sediments; however, the possibility of coexistence of highly absorbing matters such as CDOM should be considered in future stages. Measurements on the inherent optical properties (absorption and scattering), particle size distribution and other constituents (phytoplankton pigments and CDOM) are also proposed to fully understand the inter-relationship among various components and develop an analytical model to improve the ocean colour prediction in highly dynamic regions such as the Bay. Results from this experiment set the stage for in-depth regional examination of the existing and novel bio-optical models.

#### Acknowledgments

We are thankful to Dr A K S Gopalan, former Director, SAC, and Dr R R Navalgund, Director NRSA, for their unwavering encouragement and invaluable suggestions towards this work. Thanks are also due to the Dy Director General, Marine Wing, GSI, for facilitating R V *Samudra Kaustubh*, and all scientific staff and crew members onboard who helped in collecting the samples. YP thanks Dr Sam Lavender and CASIX (NERC Centre for Observation of Air-Sea Interactions and fluxes) for financial support during the preparation of this manuscript. Comments by the anonymous reviewers greatly helped to improve the original manuscript.

#### Appendix

A primary set of in-water apparent light fields can be computed from the *in situ* radiance/irradiance profiles. The different apparent optical properties (AOP) used in the creation of the CCDB were calculated from a theoretical basis (chapter 3 of Mobley 1994) and following standard protocol (Mueller 2000).

##### A.1. Diffuse attenuation coefficient for downwelling irradiance

$$K_{E_d}(z, \lambda) \cong -\frac{1}{z} \frac{\ln E_d(z, \lambda)}{\ln E_d(z_0, \lambda)} \quad (\text{A.1})$$

where  $z$  is the water depth and  $\lambda$  is the wavelength.  $E_d(z, \lambda)$  may be substituted by  $E_u(z, \lambda)$  or  $L_u(z, \lambda)$ .

For Satlantic instruments, the slope  $K$  and the intercept  $E_d(z_0)$  are calculated using a least squares first-order polynomial regression fit of the data over five regression points from the surface (data were straightened using a log (natural) transformation before the computation). However, this estimation is straightforward from LI-COR data where only discrete depth measurements are available (at 1, 5, 10 m). The  $K$  values used in this paper are integrated information over the top 5 m.

##### A.2. Water-leaving radiance

$$L_w(\lambda) = \frac{1 - \rho(\lambda, \vartheta)}{\eta_w^2(\lambda)} L_u(0^-, \lambda) \quad (\text{A.2})$$

where  $\rho$  is the Fresnel reflectance ( $\sim 0.021$ ) at the nadir angle  $\vartheta$ ,  $\eta_w$  is the refractive index of seawater ( $\sim 1.345$ ) and  $L_u(0^-, \lambda)$  is the upwelling radiance at null depth extrapolated from the profile. LI-COR measured  $E_u(z, \lambda)$  spectra can be converted to  $L_u(z, \lambda)$ , before the use of (A.2), by applying a  $Q$ -factor of 5.

##### A.3. $Q$ -factor

$$Q_n(0^-, \lambda) = \frac{E_u(0^-, \lambda)}{L_u(0^-, \lambda)} \quad (\text{A.3})$$

If the  $L_u$  distribution were isotropic, which is independent on the direction of propagation,  $Q$  would equal  $\pi$ . Actually,  $Q$  is a function of solar zenith angle and observation angle, as well as the wavelength (Morel and Gentili 1993).

#### A.4. Remote sensing reflectance

$$R_{rs}(\lambda) = \frac{L_w(\lambda)}{E_s(\lambda, 0^+)}. \quad (\text{A.4})$$

#### A.5. Downwelling surface irradiance (equivalent $E_s = (0^+, \lambda)$ )

$$E_d(0^+, \lambda) = (1 + \alpha)E_d(0^-, \lambda) \quad (\text{A.5})$$

where  $\alpha$  is the Fresnel reflection albedo from air + sky ( $\sim 0.043$ ), and  $E_d(0^-, \lambda)$  is extrapolated from the  $E_d(z, \lambda)$  profile.

#### A.6. Normalized water-leaving radiance

$$L_{wn}(\lambda) = F_0(\lambda)R_{rs}(\lambda) \quad (\text{A.6})$$

where  $F_0(\lambda)$  is the extra-terrestrial solar irradiance (from Neckel and Labs 1984).

## References

- Anonymous 2000 Test & Evaluation report on IRS-P4 OCM special product generation software *SAC Technical Report No IRS-P4/SAC/RESA/MWRD/TR/12/2000* (29 pages)
- Anonymous 2003 Atmospheric corrections, bio-optical algorithm development and validation of IRS-P4 OCM data *IRS-P4 OCM Utilisation/SATCORE Project Report* volume 1 *SAC Scientific Report No IRS-P4/SAC/RESIPA/MWRG/SR/1/2003* (150 pages)
- Austin R W and Petzold T J 1981 The determination of the diffuse attenuation coefficient of sea water using the coastal zone color scanner *Oceanography from Space* ed J F R Gower (New York: Plenum) pp 239–56
- Chauhan P 2002 personal communication
- Emmel F J and Curray J R 1984 The Bengal submarine fan-northeastern Indian ocean *Geo-Mar. Lett.* **3** 119–24
- Gordon H R, Brown O B, Evans R H, Brown J W, Smith R C, Baker K S and Clark D K 1988 A semi-analytic radiance model of ocean color *J. Geophys. Res.* **93** 10909–24
- Jerlov N G 1976 *Marine Optics* (Amsterdam: Elsevier) (231 pages)
- Laviolette P E 1967 Temperature, salinity and density of the World's Seas: Bay of Bengal and Andaman Sea *Informal Rep No 67-57* (Washington, DC: Naval Oceanographic Office)
- Lee Z P, Carder K L, Mobley C D, Steward R G and Patch J S 1998 Hyperspectral remote sensing for shallow waters. I. A semianalytical model *Appl. Opt.* **37** 6329–38
- Mobley C D 1994 *Light and Water; Radiative Transfer in Natural Waters* (London: Academic) (592 pages)
- Morel A and Gentili B 1993 Diffuse reflectance of oceanic waters II. Bidirectional aspects *Appl. Opt.* **32** 6864–79
- Morel A and Prieur L 1977 Analysis of variations in ocean color *Limnol. Oceanogr.* **22** 709–22
- Mueller J L 2000 Ocean optics protocols for satellite ocean color sensor validation, revision 2 *NASA Tech Memo 209966* ed G S Fargion and J L Mueller (Greenbelt, MD: NASA Goddard Space flight centre) chapters 8–9 pp 65–97
- Mueller J L and Austin R W 1995 Ocean optics protocols for SeaWiFS validation, revision 1 *NASA Tech Memo 104566* vol 25, ed S B Hooker, E R Firestone and J G Acker (Greenbelt, MD: NASA Goddard Space flight centre) (66 pages)
- Neckel H and Labs D 1984 The solar radiation between 3300 and 12 500 Å *Solar Phys.* **90** 205–58
- Sathyendranath S, Hoge F E, Platt T and Swift R N 1994 Detection of phytoplankton pigments from ocean color: improved algorithms *Appl. Opt.* **33** 1081–9
- Satatlantic User's Manual* 2000 (SeaWiFS Profiling Multichannel Radiometer User's Manual SPMR/SMSR 041, Issue/Rev. 1/1) (44 pages)
- Strickland J D H and Parsons T R 1972 *A Practical Handbook of Seawater Analysis* Fisheries Research Board of Canada (310 pages)
- Tassan S 1994 Local algorithms using SeaWiFS data for the retrieval of phytoplankton, pigments, suspended sediment, and yellow substance in coastal waters *Appl. Opt.* **33** 2369–78
- UNESCO 1994 Protocols for joint global ocean carbon flux study (JGOFS) core measurements *Manuals and Guides*, 29 (170 pages)